Published in final edited form as:
*J Immunol*. 2011 September 15; 187(6): 3362–3373. doi:10.4049/jimmunol.1101235.

# MicroRNA-21 limits in vivo immune response-mediated activation of the IL-12/interferon gamma pathway, Th1 polarization, and the severity of delayed-type hypersensitivity[1]

**Thomas X. Lu**[*,†,‡], **Jochen Hartner**[§,¶,‖], **Eun-Jin Lim**[*], **Victoria Fabry**[*], **Melissa K. Mingler**[*], **Eric T. Cole**[*], **Stuart H. Orkin**[§,¶], **Bruce J. Aronow**[#], and **Marc E. Rothenberg**[*,2]

[*]Division of Allergy and Immunology, Cincinnati Children's Hospital Medical Center, University of Cincinnati College of Medicine, 3333 Burnet Ave, Cincinnati, OH, 45229

[†]Graduate Program of Molecular and Developmental Biology, Cincinnati Children's Hospital Medical Center, University of Cincinnati College of Medicine, 3333 Burnet Ave, Cincinnati, OH, 45229

[‡]Physician Scientist Training Program, Cincinnati Children's Hospital Medical Center, University of Cincinnati College of Medicine, 3333 Burnet Ave, Cincinnati, OH, 45229

[§]Department of Pediatric Oncology, Dana Farber Cancer Institute, Children's Hospital, and Harvard Medical School, Boston, MA 02115

[¶]Howard Hughes Medical Institute, Boston, MA 02115

[#]Division of Biomedical Informatics, Cincinnati Children's Hospital Medical Center, University of Cincinnati College of Medicine, 3333 Burnet Ave, Cincinnati, OH, 45229

## Abstract

An altered balance between Th1 and Th2 cytokines is responsible for a variety of immuno-inflammatory disorders such as asthma, yet the role of post-transcriptional mechanisms, such as those mediated by microRNAs, in adjusting the relative magnitude and balance of Th cytokine expression have been largely unexplored. Here we show that miR-21 has a central role in setting a balance between Th1 and Th2 responses to antigens. Targeted ablation of miR-21 in mice led to reduced lung eosinophilia after allergen challenge, with a broadly reprogrammed immunoactivation transcriptome, and significantly increased levels of the Th1 cytokine IFNγ. Biological network-based transcriptome analysis of OVA-challenged miR-21$^{-/-}$mice identified an unexpected prominent dysregulation of IL-12/IFNγ pathways as the most significantly affected in the lungs with a key role for miR-21 in IFNγ signaling and T-cell polarization, consistent with a functional miR-21 binding site in *IL-12p35*. In support of these hypotheses, miR-21 deficiency led dendritic cells to produce more IL-12 after LPS stimulation, and OVA-challenged CD4$^{+}$ T lymphocytes to produce increased IFNγ and decreased IL-4. Further, loss of miR-21 significantly enhanced the Th1-associated delayed-type hypersensitivity cutaneous responses. Thus, our results

[1]This work was supported by the Ruth L. Kirschstein National Research Service Award for individual predoctoral MD/PhD fellows F30HL104892 from the National Heart Lung and Blood Institute (T.X.L), the Ryan Fellowship from Albert J. Ryan Foundation (T.X.L.), and the Organogenesis Training Grant (NIH T32HD046387 supporting T.X.L.). Targeted mice were generated in the Center for Excellence in Molecular Hematology at Children's Hospital Boston, which is supported in part by a grant from the NIDDK (P30DK049216). Additionally, this work was supported by NIH R01AI083450 (M.E.R), the Campaign Urging Research for Eosinophilic Disease (CURED); the Buckeye Foundation; and the Food Allergy Project / Food Allergy Initiative.

[2]Address correspondence to Marc E. Rothenberg, MD, PhD, Division of Allergy and Immunology, Cincinnati Children's Hospital Medical Center, 3333 Burnet Ave, ML7028, Cincinnati, OH, 45229. Phone: 513-803-0257; Fax: 513-636-3310; Rothenberg@cchmc.org.
[‖]Present address: TaconicArtemis GmbH, Cologne Area, Germany

define miR-21 as a major regulator of Th1 vs. Th2 responses, defining a new mechanism for regulating polarized immuno-inflammatory responses.

## Introduction

Th1 and Th2 cytokines oppose each other's function and typically exist in a balanced state (1). An altered balance between Th1 and Th2 cytokines is responsible for a variety of immuno-inflammatory disorders. For example, allergic inflammation is typically characterized by a Th2 cell cytokine like response, with over-expression of Th2 (e.g. IL-4, IL-5, IL-13, and IL-25) and under-expression of Th1 (e.g. IFNγ) cytokines (2, 3). While transcriptional regulation of T helper cell polarization and function has received considerable attention, the role of microRNAs (miRs) in this process has not been reported, except in an early recent report showing that let-7 regulates IL-13 expression (4), and in an elegant study showing that miR-126 suppresses the effector function of Th2 cells (5).

We have reported previously that allergic airway inflammation, triggered by allergen or IL-13,dysregulates a series of microRNAs (6). Among these microRNAs, miR-21 is the most up-regulated miR in multiple models of experimental asthma, and we found that the *IL-12p35* 3' untranslated region (UTR) contains a functional miR-21 binding site in a heterologous cell line (6). IL-12 is a major cytokine involved in Th1 cell polarization. It is a heterodimeric cytokine composed of a p35 and a p40 subunit, with the heterodimer (IL-12p70) being the bioactive protein (7). Repression of *IL-12p35* expression by miR-21 could lead to decreased IL-12p70 production and in part explain the exaggerated Th2 response seen in asthma (8). This exciting possibility, which would represent a new paradigm for controlling polarized adaptive immune responses, remains unproven given that miR-21's ability to suppress *IL-12p35* is limited to analysis in a heterologous cell line following artificial transfection and assessment of an engineered luciferase reporter construct (6). In addition, although miR-21 is strongly up-regulated following experimental asthma induction, at least twenty other microRNAs are dysregulated which could induce direct or indirect effects on a variety of complementary pathways. However, it is notable that the miR-21 binding site in the *IL-12p35* 3' UTR is conserved over a variety of species ranging from humans to platypus (6), supporting the potential of our hypothesis. The role of miR-21 will likely extend to a variety of diseases including malignancies as it is notable that miR-21 is also consistently elevated across a variety of tumors (9).

In this study we sought to determine the *in vivo* impact of miR-21 on murine models of hypersensitivity in the lung and skin using a novel strain of miR-21 gene-targeted mice. We first identified mRNA transcripts dysregulated in the lung during allergic inflammation by loss of miR-21. We then used an unbiased systems biology analysis approach that identified an unexpected prominent dysregulation of IL-12/IFNγ pathways as the most significantly affected in the lungs of OVA-challenged miR-21$^{-/-}$ mice compared to miR-21$^{+/+}$ littermates. In turn, miR-21 deficient mice had increased IFNγ and decreased IL-4 levels in the lung compared to wild-type littermates. This was associated with reduced eosinophilia in the lungs of miR-21$^{-/-}$ mice. To test for the cellular origins of these effects, we next demonstrated that miR-21$^{-/-}$ dendritic cells produced significantly more IL-12 compared to wild-type dendritic cells after LPS stimulation, potentiated by IFNγ co-stimulation. Furthermore, OVA-challenged miR-21$^{-/-}$ CD4$^{+}$ T lymphocytes produced increased IFNγ and decreased IL-4 compared to control cells. To broaden our finding, we examined the impact of miR-21 deficiency in an independent, Th1-associated cutaneous delayed-type hypersensitivity model. We demonstrated that the loss of miR-21 significantly enhanced the Th1-associated cutaneous delayed-type hypersensitivity responses. These data demonstrate that miR-21 has a central role in establishing the fine balance of Th1 vs. Th2 responses to

antigens and suggest that targeting miR-21 and understanding variations in its activity may lead to new treatments and preventions for a variety of diseases that exhibit dysregulated Th1/Th2 balance such as allergic asthma.

## Material and Methods

### MiR-21 gene targeting

The pFlexible-based miR-21 gene-targeting vector (10), modified to permit diphtheria toxin A negative selection in embryonic stem (ES) cells, contained 6.3 kb of 5' homologous sequence including exon 12 of the *Tmem49* (*VMP1*) gene, 1.4 kb of loxP-flanked sequence containing pre-miR-21, and a Flp recombinase recognition (FRT) site-flanked *pgk-puroΔTK* gene, followed by 1.5 kb of 3' homologous sequence. Homologous and conditional miR-21 sequence was amplified from CJ7 ES cell-derived genomic DNA by PCR and verified by DNA sequencing. The linearized targeting vector was electroporated into CJ7 ES cells, and PCR-mediated screening of 114 puromycin-resistant cells yielded 31 candidates. Correct homologous recombination in three candidate ES cell clones was confirmed by Southern analysis and locus-specific PCR selectively amplifying the targeted miR-21 allele combined with DNA sequencing. Two independently targeted ES cell clones were injected into C57BL/6 derived blastocysts, and chimeric offspring were bred with C57BL/6 EIIA-Cre mice to delete the pre-miR-21 containing conditional sequence. Germline deletion of the conditional miR-21 allele was demonstrated by genomic PCR in heterozygous mice that had been backcrossed to remove the *cre* transgene. Heterozygous intercrosses yielded homozygous mice at the expected Mendelian frequency. Mouse lines derived from two independently targeted ES cell clones were phenotypically indistinguishable. The mice were backcrossed for two generations into the C57BL/6 background for the murine asthma models. The mice were backcrossed for five generations into the C57BL/6 background for the delayed-type hypersensitivity experiments. Littermate controls were used for all experiments. All animals used were housed under specific pathogen-free conditions in accordance with institutional guidelines. The Institutional Animal Care and Use Committee of the Cincinnati Children's Hospital Medical Center approved the use of animals in these experiments.

### Northern analyses

Total RNA from wild-type miR-21$^{+/+}$, heterozygous conditional miR-21$^{f/+}$, and homozygous gene-targeted miR-21$^{-/-}$ CJ7 ES cells was extracted using standard procedures. For miRNA expression analysis, 20 μg of total RNA per sample were electrophoretically separated on a 15% polyacrylamide TBE/urea gel and transferred to a nylon membrane via semi-dry transfer. Expression of miR-21, miR-294, and 5S RNA was detected by sequentially hybridizing the membrane with radioactively labeled DNA oligonucleotide probes. For mRNA expression analysis, 30 μg of denatured total RNA per sample were electrophoretically separated on a 1.2 % [w/v] agarose gel and transferred to a nylon membrane via alkaline downward capillary transfer. Expression of *Tmem49* (*VMP1*) and *GAPDH* mRNA was detected by sequential hybridization of the membrane with radioactively labeled DNA probes.

### Experimental asthma induction

Experimental asthma was induced by injection with 100 μg OVA and 1 mg aluminum hydroxide as adjuvant on day 0 and day 10, followed by 50 μg OVA or saline intranasal challenges on day 20, 21, and 22. Mice were sacrificed 18-24 hours after the last challenge (11).

### Bronchoalveolar lavage fluid (BALF) collection and analysis

BALF was collected according to previously published methods (12). Total cell numbers were counted with a hemacytometer. Cytospin preparations of $7.5 \times 10^4$ cells were stained with Diff-Quik solution, and differential cell counts were determined using standard morphological criteria. At least 250 cells were counted per slide for differential cell counts. Cytokine levels of IFNγ, IL-4 and CXCL9 were determined using the Milliplex Multi-Analyte Profiling Immunoassay (Millipore). Levels of CCL17 were determined using DuoSet ELISA kits (R&D Systems) according to manufacturer's protocol.

### Quantification of eosinophil infiltration in the lung

Quantification of eosinophil infiltration in the lung tissue was performed as previously described (12). Briefly, lung tissue eosinophils were identified by anti-major basic protein staining. Quantification of immunoreactive cells was performed by counting the positive-stained cells under low-power magnification, and eosinophil levels were expressed as the number of eosinophils per square millimeter.

### Quantitative assessment of miR levels

Total RNA was isolated using the miRNeasy Mini Kit (Qiagen) according to manufacturer's protocol. Levels of miR expression were measured quantitatively by using the TaqMan MicroRNA Assay (Applied Biosystems) following the manufacturer's protocol and assayed on the Applied Biosystems 7900HT Real-Time PCR System (13). Normalization was performed using U6 small nuclear RNA. Relative expression was calculated using the comparative $C_T$ method as previously described (14).

### qRT-PCR

Total RNA was reverse transcribed using the High Capacity cDNA Reverse Transcription kit (Applied Biosystems). All primer/probe sets were obtained from Applied Biosytems. Samples were analyzed by TaqMan qRT-PCR for IL-12p35 (Assay ID: Mm00434169_m1), IFNγ (Assay ID: Mm_00801778_m1), CXCL10 (Assay ID: Mm_00445235_m1), and normalized to *HPRT1* (Assay ID: Mm00446968_m1). Relative expression was calculated using the comparative $C_T$ method (14).

### Culture of bone marrow derived dendritic cells

Bone marrow derived dendritic cells were prepared by culturing cells in RPMI-1640 medium supplemented with 40 ng/mL GM-CSF, 10 ng/mL IL-4, 10% FBS, 1% penicillin/streptomycin, and 50 μM β-mercaptoethanol for 7 days as previously described (15).

### Measurement of cytokine production from bone marrow derived dendritic cells

Bone marrow derived dendritic cells were stimulated with 1 μg/mL LPS (Strain: 055:B5, Sigma) or 1 μg/mL LPS + 100 IU/mL of IFNγ (eBioscience) for 48 hours. IL-12p70 concentrations from cell culture supernatants were measured using the Legend Max Mouse IL-12p70 ELISA Kit (Biolegend) according to the manufacturer's protocol. TNFα and IL-6 concentrations from cell culture supernatants were measured using ELISA Max Deluxe kits (Biolegend) according to the manufacturer's protocol. To measure the levels of IL-23 production, bone marrow derived dendritic cells were stimulated with 1 μg/mL LPS for 12, 24 or 48 hrs. IL-23 concentrations from cell culture supernatants were measured using IL-23 DuoSet ELISA kit (R&D Systems) according to manufacturer's protocol. To measure the levels of IFNγ production, bone marrow derived dendritic cells were stimulated with 10 ng/mL IL-12, 10 ng/mL IL-23 or 1 μg/mL LPS for 48 hrs. IFNγ concentrations from cell culture supernatants were measured using IFNγ ELISA Ready-Set-Go kit (eBioscience) according to manufacturer's protocol.

### Gene expression microarray analysis

Total RNA was isolated from lung tissue using the miRNeasy Mini Kit according to the manufacturer's protocol (Qiagen). RNA quality was assessed by using the Agilent 2100 bioanalyzer (Agilent Technologies), and only samples with an RNA integrity number > 8 were used. Microarray analysis was performed as previously described (11). The Affymetrix mouse Gene 1.0ST array was used, and data were analyzed using GeneSpring software (Agilent Technologies). Global scaling was performed to compare genes from chip to chip, and a base set of probes was generated by requiring a minimum raw expression level of $20^{th}$ percentile out of all probes on the microarray. To identify miR-21 regulated genes, the probe sets were then baseline transformed and filtered on at least a 1.2-fold change between miR-$21^{+/+}$ and miR-$21^{-/-}$ mice in either saline- or OVA-challenged mice. A cut off of 1.2 fold was selected because miRs are currently reported to have only mild to moderate effects on gene expression, with some targets repressed without detectable change in mRNA levels (16, 17). Statistical significance was determined at $p < 0.05$ with Benjamini Hochberg false discovery rate correction. The resulting list of genes was clustered using hierarchical clustering and a heatmap was generated. Pathway analysis of differentially regulated genes was carried out using Ingenuity Pathway Analysis (Ingenuity Systems) and Toppgene/ Toppcluster (18). The microarray data have been deposited into the Array Express database (www.ebi.ac.uk/arrayexpress) with accession number E-MEXP-3119 in compliance with minimum information about microarray experiment (MIAME) standards.

### Analysis of human samples for miR-21 expression patterns

Global human transcriptome analysis of miR-21 expression patterns were carried out using two large human Affymetrix gene expression datasets, one based on a series of more than 2000 human cancers (the Cancer ExPO database NCBI GSE2109, and the other the Human Body Index, GSE7307, that contains 677 samples representing over 90 human tissue samples and isolated cell types. CEL files were subjected to RMA normalization, and then transformed into a normalized matrix representing the relative expression of each probe across each of the two large datasets. The data were then analyzed by Pearson correlation analyses to identify probesets on the HG U-133 plus 2.0 gene chip that were regulated most similarly to the Affymetrix probeset 224917_at that we had predicted would be the best indicator of miR-21 host gene RNA expression. Functional enrichment analysis of the gene list were carried out using the Toppgene suite (19).

### Isolation and re-stimulation of $CD4^+$ T lymphocytes from spleen

Splenic $CD4^+$ T cells were isolated using $CD4^+$ T cell isolation kit II (Miltenyi Biotec) according to the manufacturer's protocol. The $CD4^+$ T cells were then re-stimulated with Dynabeads Mouse T-Activator CD3/CD28 (Invitrogen) according to the manufacturer's protocol. Supernatants were collected after 72 hours, and concentrations of IFNγ and IL-4 were measured using ELISA Max deluxe kits (Biolegend) according to the manufacturer's protocol.

### Isolation and re-stimulation of total splenocytes

Isolation and re-stimulation of total splenocytes were performed as previously described (20).Briefly, spleens were aseptically removed from mice. Single-cell suspensions were obtained by mincing the spleen and gently pressing the fragments through a 70μm filter. The cell suspensions were washed twice in Advanced RPMI 1640 medium supplemented with 10% FBS, 2 mM L-glutamine, 1 mM sodium pyruvate, 50 U/mL penicillin, and 50 μg/ml streptomycin. After counting by trypan blue exclusion, they were adjusted to a density of $1\times10^7$ cells/mL. Cells were plated at 1 mL/well in 24 well cell culture plates and challenged with OVA at a final concentration of 100 μg/mL or with an equivalent volume of saline.

Supernatants were collected after 72 hours, and concentrations of IFNγ and IL-4 were measured using ELISA Max deluxe kits (Biolegend) according to the manufacturer's protocol.

### Isolation and stimulation of NK cells

Splenic NK cells were isolated using NK Cell Isolation Kit (Miltenyi Biotec) according to the manufacturer's protocol. The NK cells were then stimulated with 10 ng/mL IL-12. Supernatants were collected after 48 hours, and concentrations of IFNγ were measured using ELISA Max deluxe kits (Biolegend) according to the manufacturer's protocol.

### NP-OSu-mediated delayed-type hypersensitivity reaction

NP-OSu-mediated delayed-type hypersensitivity was induced by immunizing 9-12 weeks old miR-21$^{+/+}$ and miR-21$^{-/-}$ mice subcutaneously in two sites, one on each ventral flank, with 50 μL of 2.5% 4-hydroxy-3-nitrophenylacetyl-hydroxysuccinimide ester (NP-OSu; Biosearch Technologies) dissolved in dimethyl sulfoxide, followed by subcutaneous injection of 100 μL of 1X borate-buffered saline (pH 8.6) in the dorsal midline. Six days later, the left rear footpad was challenged with 25 μL of 2.5% NP-OSu freshly diluted 1:20 in PBS (pH 7.8). Control mice were sensitized with DMSO and challenged with NP-OSu solution. The left and right footpad thickness was quantified 24 hours after the challenge by using a digital micrometer with 0.01 mm resolution (Mitutoyo). After euthanasia, the left and right rear paws were removed uniformly at the ankle joint and weighed. NP-OSu-induced increases in footpad thickness or weight were calculated by subtracting the right footpad thickness or weight from that of the left footpad.

### Statistical Analysis

Statistical analyses were performed with student's *t*-test or one-way ANOVA with Tukey post-hoc test where appropriate. Statistical significance and the p values were indicated on the figures where appropriate. P values less than 0.05 were considered statistically significant.

## Results

### Generation of miR-21$^{-/-}$ mice

Targeted disruption of the miR-21 coding sequence was carried out as shown in Figure 1A. Deletion of miR-21 coding sequence was confirmed by northern blot and PCR analyses (Fig. 1B-C). Regulatory sequences of miR-21 were located adjacent to the *Tmem49* gene (also known as *VMP1*). *Tmem49* mRNA expression was unaltered in miR-21$^{-/-}$ mice (Fig. 1D). MiR-21$^{-/-}$ mice appeared indistinguishable from their wild-type and heterozygous littermates and were delivered in expected Mendelian ratios (n > 100), as recently reported in an independent miR-21$^{-/-}$ mouse strain (21).

### Gene expression microarray analysis identifies a subset of allergic airway inflammation signature genes that are regulated by miR-21

To identify genes whose regulation was affected by the absence or presence of miR-21 in normal or immune-challenged conditions, we performed gene expression microarray analyses of RNA from lungs of saline- and OVA-challenged miR-21$^{+/+}$ and miR-21$^{-/-}$ mice. At baseline, using a statistical cutoff of $p < 0.05$ and > 1.2-fold difference, there were 54 gene-associated transcripts that exhibited differential expression between miR-21$^{+/+}$ mice and miR-21$^{-/-}$ mice (Supplemental Table 1). Following OVA challenge, miR-21$^{+/+}$ and miR-21$^{-/-}$ mice both exhibited robust induction of allergen associated gene signatures. Post-hoc filtering to identify allergen response transcripts most significantly affected by the loss

of miR-21 identified 316 probe sets that differed by greater than 1.2 fold at $p < 0.05$ (Supplemental Table 2). These included 37 of the 54 saline baseline-affected probes that were also similarly affected under OVA challenge conditions. Hierarchical cluster analysis of the differentially expressed genes identified four striking clusters of differentially expressed genes between miR-21$^{+/+}$ and miR-21$^{-/-}$ mice (Fig.2A): miR-21$^{-/-}$ hyper-activated, with notable enrichment for IFNγ signature genes; miR-21$^{-/-}$ de-activated and miR-21$^{-/-}$ hyper-repressed, which include Th2-associated genes such as the chemokine CCL17 (22); and miR-21$^{-/-}$ de-repressed, including IL-18, which is associated with Th1 and Th2 response (Fig. 2A) (23, 24). A full list of genes in these four clusters can be found in Supplemental Table 2.

## Pathway analysis revealed striking effects by miR-21 on IL-12 and IFNγ associated pathways

Genes that were differentially regulated by miR-21 were then analyzed using Ingenuity Pathway Analysis. The most significant alteration of all pathways was up-regulation of IL-12 and IFNγ dependent networks in miR-21$^{-/-}$ mice compared to miR-21$^{+/+}$ littermates (Fig.2B). The individual nodes in the pathway including genes and/or gene categories identified by the Ingenuity Pathway Analysis are listed in Supplemental Table 3. In order to better understand the potential molecular basis and consequences of the dysregulated IL-12/IFNγ pathway, we performed biological network analyses using Toppcluster, a multiple gene list feature analyzer for comparative enrichment clustering and network-based dissection of biological systems (Fig. 2C) (18). Unlike the Ingenuity Pathway Analysis approach that is focused on gene and protein interactions, Toppcluster enables connections to be made between genes and gene-associated features that encompass the positive functions of genes (e.g. participation in a pathway, biological process, protein-protein interactions), regulatory mechanisms via transcription factors or miRNAs, and the consequences of loss of gene functions as evidenced by mouse or human disease phenotypes. This approach provided further insight into relationships among the miR-21$^{-/-}$ dysregulated genes relative to IFNγ signaling and responses, and highlighted the extensive up-regulation of genes that are either positive activators of IFNγ signaling or its downstream effectors. For example, targeted gene disruption of several of these over-expressed genes give phenotypes in mice that cause decreased IFNγ production and/or increased IL-4 expression (Fig. 2C).

In conjunction with our prior demonstration that miR-21 has the capacity to directly target the *IL-12p35* 3' UTR based on a luciferase reporter assay in heterologous cell *in vitro* (6), these results and global systems biological analyses demonstrate that in the midst of a complex large-scale allergic airway hypersensitivity immune response, the impact of miR-21 exerts a strong polarizing role in modifying the effects of cardinal immune activation pathways.

## MiR-21 polarizes Th2 cytokine production in the lung after allergen challenge

To test the impact of miR-21 on the levels of Th1 and Th2 cytokines generated by the lung in response to allergen-challenge, bronchoalveolar lavage fluid (BALF) of miR-21 deficient mice were compared to wild-type littermate controls. Consistent with the results from our systems biology analysis, miR-21$^{-/-}$ mice had increased levels of the Th1 cytokine IFNγ as well as CXCL9, a chemokine known to be induced by IFNγ (Fig. 3A-B) (25), and decreased levels of the Th2-associated cytokines IL-4 and CCL17 (Fig. 3C-D) (26). We also measured the levels of IL-12p35 by quantitative real-time PCR (qRT-PCR) and found increased levels of IL-12p35 in the miR-21 deficient mice compared to wild-type littermate controls (Fig. 3E).

### MiR-21$^{-/-}$ mice have reduced eosinophilia in the lung after allergen challenge

Based on the strong down-regulation of multiple eosinophil specific transcripts and Th2-associated chemokines in the microarray data, we questioned whether the loss of miR-21 caused loss of eosinophils in the lung. MiR-21$^{-/-}$ mice had significantly reduced levels of eosinophil infiltration in the BALF after allergen challenge compared with wild-type littermate controls (Fig.4A), with correspondingly reduced eosinophil percentages in the BALF (Fig.4B) and reduced eosinophil level in the lung tissue (Fig.4C). These results indicate that the increased IFNγ polarization had functional and specific consequences, as the levels of neutrophils, lymphocytes, and macrophages were not significantly changed in the BALF (Fig.4A).

### Dendritic cells from miR-21$^{-/-}$ mice produced increased IL-12p70 after LPS stimulation in the presence or absence of IFNγ co-stimulation

To find a mechanistic basis of the increased Th1 response in the miR-21 deficient mice after allergen challenge, we cultured bone marrow derived dendritic cells from miR-21$^{+/+}$ and miR-21$^{-/-}$ mice, and stimulated the dendritic cells with LPS alone or LPS plus IFNγ. We then measured the levels of IL-12p70 in the supernatant. Compared to dendritic cells from wild-type littermates, dendritic cells from miR-21 deficient mice produced significantly increased levels of IL-12p70 after LPS or LPS/IFNγ stimulation (Fig.5A). By contrast, there was no change in the levels of TNFα or IL-6 produced, demonstrating specificity of the increased IL-12p70 production by miR-21 deficient dendritic cells (Fig. 5B-C). Since IL-23 production from dendritic cells is also an important regulator of Th1 vs. Th2 balance, we measured the levels of IL-23 production from bone marrow derived dendritic cells after 12, 24 or 48 hrs of LPS stimulation. The bone marrow derived dendritic cells produced maximum amounts of IL-23 after 12 hrs of LPS stimulation, consistent with previous reports in the literature (27). However, compared to dendritic cells from wild-type littermates, dendritic cells from miR-21 deficient mice produced similar levels of IL-23 after 12, 24 or 48 hrs of LPS stimulation (Fig. 5D).

### Splenic CD4$^{+}$ T cells from miR-21$^{-/-}$ mice produced increased IFNγ and decreased IL-4 compared to cells from wild-type littermates

To further support the hypothesis that miR-21 regulates Th1 vs. Th2 responses, we compared cytokine responses in isolated CD4$^{+}$ T cells from spleens of OVA-challenged miR-21$^{-/-}$ mice and wild-type controls. Compared to the wild-type littermate controls, anti-CD3/CD28 re-stimulated CD4$^{+}$ T cells from miR-21$^{-/-}$ mice produced increased IFNγ and decreased IL-4, with a correspondingly increased IFNγ/IL-4 ratio (Fig. 6A-C). Re-stimulation of total splenocytes from OVA-challenged mice with OVA showed similar results (Fig. 6D-E). By contrast, anti-CD3/CD28 re-stimulated CD4$^{+}$ T cells from naïve miR-21$^{-/-}$ mice produced similar levels of IFNγ and IL-4 as the naïve wild-type littermates (Fig. 6F-G)

### IFNγ production by NK cells and dendritic cells from miR-21$^{-/-}$ mice compared to wild-type littermates

Since NK cells and dendritic cells are also important IFNγ producing cells, we measured the levels of IFNγ production by IL-12 stimulated NK cells from spleen and IL-12, IL-23 or LPS stimulated bone marrow derived dendritic cells. IL-12 stimulated NK cells from miR-21$^{-/-}$ mice produced similar amounts IFNγ as NK cells from wild-type littermates (Fig. 7A). IL-12 stimulated dendritic cells from miR-21$^{-/-}$ mice also produced similar amounts IFNγ as dendritic cells from wild-type littermates (Fig. 7B). The levels of IFNγ produced by the dendritic cells after IL-23 stimulation were below detection limit (Fig. 7B). The LPS stimulated dendritic cells from miR-21 deficient mice produced significantly increased

levels of IFNγ compared to dendritic cells from wild-type littermates (Fig. 7B), likely because of the increased IL-12p70 production from miR-21 deficient dendritic cells after LPS stimulation (Fig. 5A).

### MiR-21$^{-/-}$ mice have enhanced delayed-type hypersensitivity cutaneous response compared to miR-21$^{+/+}$ littermate controls

We aimed to broaden our findings by testing whether miR-21 had a role in regulating IL-12/IFNγ responses in another tissue outside the lung and also in a distinct, non-allergic model, characterized by polarized Th1-responses. Accordingly, we utilized an NP-OSu-induced Th1 cytokine-associated model of delayed-type hypersensitivity in the skin (28). In this model, sensitized mice were challenged by footpad injection of NP-OSu. Compared to wild-type littermate controls, miR-21$^{-/-}$ mice had an increase in footpad thickness and footpad weight, indicative of an increased footpad swelling response in these mice (Fig. 8A-B). This was accompanied by an increase in IFNγ mRNA in the footpad, with a corresponding increase in the IFNγ-induced chemokine CXCL10 (Fig. 8C-D) (29).

## Discussion

Herein, we provide definitive evidence that the main function of miR-21 is to regulate IL-12/IFNγ axis in multiple models of immune hypersensitivity and that the role of miR-21 in this process is non-redundant. Notably, we provide empiric evidence that this is a major and functionally relevant role for miR-21. To the best of our knowledge, this is the first study demonstrating the role of miR-21 in regulating Th1 vs. Th2 responses *in vivo*. Prior studies concerning miR-21 have primarily focused on its role in tumorigenesis and tissue remodeling (21, 30-33), so the finding that miR-21 dominantly regulates the IL-12/IFNγ axis *in vivo* is unexpected. Prior work concerning the regulation of IL-12/IFNγ has all focused on their molecular regulation by cytokines and transcription factors (7, 34), so our finding that this critical step in adaptive immunity is regulated by a specific microRNA presents a new paradigm with broad and deep implications.

We have previously shown that miR-21 is the most up-regulated miR in multiple models of experimental allergic airway inflammation (6), a finding verified by a recent report from the laboratory of Dr. Paul Foster (5). We previously proposed that miR-21 targets *IL-12p35* based on predictive algorithms and *in vitro* studies using reporter systems in heterologous cells. However, the *in vivo* function of miR-21 in the setting of natural adaptive immune responses had not been established, especially in light of the myriad of microRNAs dysregulated during allergic airway inflammation. It is also well known that microRNA predictive algorithms have limitations, including lack of specificity as single microRNAs have the capacity to directly target a myriad of mRNAs. This is illustrated in part by the recent report that miR-21 deficient mice have no alteration in cardiac remodeling even though this outcome was expected based on predictive algorithms and antagomir studies (21, 30).

IL-12 is a major cytokine that regulates Th1 vs. Th2 decisions primarily by inducing T cells to produce the Th1 cytokine IFNγ (7). Using gene expression microarray and systems biology analysis, we identified an IL-12/IFNγ dependent pathway as the most prominent up-regulated pathway in the lungs of OVA-challenged miR-21$^{-/-}$ mice compared to wild-type littermate controls, providing substantial evidence that this is the major pathway dysregulated in the miR-21 deficient mice. We then demonstrated that the miR-21 deficient mice have increased levels of the Th1 cytokine IFNγ and relevant IFNγ-induced genes, such as CXCL9, after allergen challenge compared to wild-type littermates. CD4$^{+}$ T cells from OVA-challenged miR-21$^{-/-}$ mice produced increased levels of IFNγ and reduced levels of IL-4 compared to cells from wild-type littermates following OVA or anti-CD3/CD28

stimulation, indicating the functional consequences of IL-12 production on subsequent T cell responses. By contrast, naïve $CD4^+$ T cells from miR-21 deficient mice produced similar levels of IFNγ and IL-4 compared to cells from wild-type littermates following anti-CD3/CD28 stimulation, indicating that the Th1 skewed response in miR-$21^{-/-}$ mice is likely due to increased IL-12 production. Indeed, bone marrow-derived dendritic cells from miR-21 deficient mice produced significantly more IL-12p70 compared to control mice, thus providing a mechanistic basis for the experimental asthma phenotype seen in the miR-$21^{-/-}$ mice. Since NK cells and dendritic cells are also important IFNγ producing cells, we measured the levels of IFNγ production by NK cells and dendritic cells from miR-21 deficient mice compared to wild-type littermates. The NK cells and dendritic cells from miR-21 deficient mice produced similar amounts of IFNγ compared to wild-type littermates following IL-12 stimulation, further supporting our hypothesis that the Th1 skewed response in miR-$21^{-/-}$ mice is due to increased IL-12 production. The LPS stimulated dendritic cells from miR-21 deficient mice produced significantly increased levels of IFNγ compared to dendritic cells from wild-type littermates, likely because of the increased IL-12p70 production from miR-21 deficient dendritic cells after LPS stimulation.

We evaluated the applicability of these findings in an independent system *in vivo* by examining the Th1-dependent,delayed-type hypersensitivity cutaneous response in miR-21 deficient mice. Interestingly, miR-21 deficient mice had an enhanced delayed-type hypersensitivity response characterized by increased footpad swelling and IFNγ level in the footpad. Thus, we propose that miR-21 mediated attenuation of the IL-12/IFNγ pathway has profound effects on regulating adaptive immune responses. These findings underscore the sensitivity of Th1 vs. Th2 decisions and identify a key role for miRNA-mediated post-transcriptional regulation of this process.

Our findings do not preclude the possibility that miR-21 may regulate multiple other pathways. Abundant evidence points to the role of miR-21 in regulating anti-apoptosis pathways, particularly those involved in oncogenesis, by targeting genes such as programmed cell death 4 (PDCD4) and phosphatase and tensin homology deleted from chromosome 10 (PTEN), which have also been implicated in immunity (35-38). To consider the potential significance of miR-21 in the polarization of the immune-inflammatory responses in normal and cancerous tissues, we evaluated miR-21 expression in two large human Affymetrix gene expression datasets, one based on a series of more than 2,000 human cancers (the Cancer ExPO database NCBI GSE2109, compiled by the international genomics consortium) and the other based on the Human Body Index, GSE7307, that contains 677 samples representing over 90 distinct human tissue types. We identified the Affymetrix probe set 224917_at as the best potential indicator of miR-21 gene expression and used Pearson correlation analysis across the cancer set to identify 269 probesets corresponding to 182 human genes whose pattern of expression was highly similar to that of the miR-21 host gene (Supplemental Table 4). Of these, 245 probe sets maintained a correlation level greater than 0.2 in the normal human body map. Tissues that exhibited a high level of miR-21 expression included many mucosal epithelium-containing tissues such as lung and oral mucosa as well as the lymphoid tissues spleen, tonsil, and lymph nodes. Remarkable similarities were also identified between the human signature and mouse pathways, with both being enriched in immuno-inflammatory processes (Table 1). It is notable that a large-scale survey to determine the miRNA signature of 540 diverse tumor samples identified miR-21 as the only miRNA up-regulated in all of these tumors (9); and miR-21 has been recently shown to be a true oncomiR (31, 32). Given that Th2 responses have recently been shown to be tumorigenic (39, 40), the ability of miR-21 to promote a Th2 vs. Th1 microenvironment may be an additional mechanism for its oncogenic effects.

In summary, we have identified miR-21 as a regulator of the polarization of Th1/Th2 responses in multiple models of immuno-inflammatory hypersensitivity. We propose that despite the multistep nature of adaptive immune responses and the number of regulatory steps involved, Th1 vs. Th2 decisions appear to be miR-21 dependent. The presented findings have broad implications for diseases associated with imbalanced Th1 and Th2 responses (e.g. asthma) and other diseases associated with miR-21 overexpression (e.g. cancer). Thus, targeting miR-21 and understanding variations in its activity and impact on the IL-12/IFNγ pathway may lead to potentially far-reaching treatments and preventions. Taken together, our findings provide a new mechanism for regulating a critical arm of adaptive polarized immune responses.

## Supplementary Material

Refer to Web version on PubMed Central for supplementary material.

## Acknowledgments

We would like to thank Shawna K.B. Hottinger for editorial assistance.

## References

1. Romagnani S. Immunologic influences on allergy and the TH1/TH2 balance. J Allergy Clin Immunol. 2004; 113:395–400. [PubMed: 14758340]
2. Kim HY, DeKruyff RH, Umetsu DT. The many paths to asthma: phenotype shaped by innate and adaptive immunity. Nat Immunol. 2010; 11:577–584. [PubMed: 20562844]
3. Hamid Q, Tulic M. Immunobiology of asthma. Annu Rev Physiol. 2009; 71:489–507. [PubMed: 19575684]
4. Polikepahad S, Knight JM, Naghavi AO, Oplt T, Creighton CJ, Shaw C, Benham AL, Kim J, Soibam B, Harris RA, Coarfa C, Zariff A, Milosavljevic A, Batts LM, Kheradmand F, Gunaratne PH, Corry DB. Proinflammatory role for let-7 microRNAS in experimental asthma. J Biol Chem. 2010; 285:30139–30149. [PubMed: 20630862]
5. Mattes J, Collison A, Plank M, Phipps S, Foster PS. Antagonism of microRNA-126 suppresses the effector function of TH2 cells and the development of allergic airways disease. Proc Natl Acad Sci U S A. 2009; 106:18704–18709. [PubMed: 19843690]
6. Lu TX, Munitz A, Rothenberg ME. MicroRNA-21 is up-regulated in allergic airway inflammation and regulates IL-12p35 expression. J Immunol. 2009; 182:4994–5002. [PubMed: 19342679]
7. Gately MK, Renzetti LM, Magram J, Stern AS, Adorini L, Gubler U, Presky DH. The interleukin-12/interleukin-12-receptor system: role in normal and pathologic immune responses. Annu Rev Immunol. 1998; 16:495–521. [PubMed: 9597139]
8. Larche M, Robinson DS, Kay AB. The role of T lymphocytes in the pathogenesis of asthma. J Allergy Clin Immunol. 2003; 111:450–463. [PubMed: 12642820]
9. Volinia S, Calin GA, Liu CG, Ambs S, Cimmino A, Petrocca F, Visone R, Iorio M, Roldo C, Ferracin M, Prueitt RL, Yanaihara N, Lanza G, Scarpa A, Vecchione A, Negrini M, Harris CC, Croce CM. A microRNA expression signature of human solid tumors defines cancer gene targets. Proc Natl Acad Sci U S A. 2006; 103:2257–2261. [PubMed: 16461460]
10. van der Weyden L, Adams DJ, Harris LW, Tannahill D, Arends MJ, Bradley A. Null and conditional semaphorin 3B alleles using a flexible puroDeltatk loxP/FRT vector. Genesis. 2005; 41:171–178. [PubMed: 15789413]
11. Zimmermann N, King NE, Laporte J, Yang M, Mishra A, Pope SM, Muntel EE, Witte DP, Pegg AA, Foster PS, Hamid Q, Rothenberg ME. Dissection of experimental asthma with DNA microarray analysis identifies arginase in asthma pathogenesis. J Clin Invest. 2003; 111:1863–1874. [PubMed: 12813022]
12. Fulkerson PC, Fischetti CA, Hassman LM, Nikolaidis NM, Rothenberg ME. Persistent effects induced by IL-13 in the lung. Am J Respir Cell Mol Biol. 2006; 35:337–346. [PubMed: 16645178]

13. Chen C, Ridzon DA, Broomer AJ, Zhou Z, Lee DH, Nguyen JT, Barbisin M, Xu NL, Mahuvakar VR, Andersen MR, Lao KQ, Livak KJ, Guegler KJ. Real-time quantification of microRNAs by stem-loop RT-PCR. Nucleic Acids Res. 2005; 33:e179. [PubMed: 16314309]
14. Livak KJ, Schmittgen TD. Analysis of relative gene expression data using real-time quantitative PCR and the 2(-Delta Delta C(T)) Method. 2001; 25:402–408.
15. Mayordomo JI, Zorina T, Storkus WJ, Zitvogel L, Garcia-Prats MD, DeLeo AB, Lotze MT. Bone marrow-derived dendritic cells serve as potent adjuvants for peptide-based antitumor vaccines. Stem Cells. 1997; 15:94–103. [PubMed: 9090785]
16. Baek D, Villen J, Shin C, Camargo FD, Gygi SP, Bartel DP. The impact of microRNAs on protein output. Nature. 2008; 455:64–71. [PubMed: 18668037]
17. Selbach M, Schwanhausser B, Thierfelder N, Fang Z, Khanin R, Rajewsky N. Widespread changes in protein synthesis induced by microRNAs. Nature. 2008; 455:58–63. [PubMed: 18668040]
18. Kaimal V, Bardes EE, Tabar SC, Jegga AG, Aronow BJ. ToppCluster: a multiple gene list feature analyzer for comparative enrichment clustering and network-based dissection of biological systems. Nucleic Acids Res. 2010; 38:W96–102. [PubMed: 20484371]
19. Chen J, Bardes EE, Aronow BJ, Jegga AG. ToppGene Suite for gene list enrichment analysis and candidate gene prioritization. Nucleic Acids Res. 2009; 37:W305–311. [PubMed: 19465376]
20. Sakai S, Akiyama H, Harikai N, Toyoda H, Toida T, Maitani T, Imanari T. Effect of chondroitin sulfate on murine splenocytes sensitized with ovalbumin. Immunol Lett. 2002; 84:211–216. [PubMed: 12413739]
21. Patrick DM, Montgomery RL, Qi X, Obad S, Kauppinen S, Hill JA, van Rooij E, Olson EN. Stress-dependent cardiac remodeling occurs in the absence of microRNA-21 in mice. J Clin Invest. 2010; 120:3912–3916. [PubMed: 20978354]
22. Romagnani S. Cytokines and chemoattractants in allergic inflammation. Mol Immunol. 2002; 38:881–885. [PubMed: 12009564]
23. Kang MJ, Homer RJ, Gallo A, Lee CG, Crothers KA, Cho SJ, Rochester C, Cain H, Chupp G, Yoon HJ, Elias JA. IL-18 is induced and IL-18 receptor alpha plays a critical role in the pathogenesis of cigarette smoke-induced pulmonary emphysema and inflammation. J Immunol. 2007; 178:1948–1959. [PubMed: 17237446]
24. Calvani N, Tucci M, Richards HB, Tartaglia P, Silvestris F. Th1 cytokines in the pathogenesis of lupus nephritis: the role of IL-18. Autoimmun Rev. 2005; 4:542–548. [PubMed: 16214093]
25. Farber JM. A macrophage mRNA selectively induced by gamma-interferon encodes a member of the platelet factor 4 family of cytokines. Proc Natl Acad Sci U S A. 1990; 87:5238–5242. [PubMed: 2115167]
26. Wirnsberger G, Hebenstreit D, Posselt G, Horejs-Hoeck J, Duschl A. IL-4 induces expression of TARC/CCL17 via two STAT6 binding sites. Eur J Immunol. 2006; 36:1882–1891. [PubMed: 16810739]
27. Chang J, Voorhees TJ, Liu Y, Zhao Y, Chang CH. Interleukin-23 production in dendritic cells is negatively regulated by protein phosphatase 2A. Proc Natl Acad Sci U S A. 2010; 107:8340–8345. [PubMed: 20404153]
28. Lu B, Rutledge BJ, Gu L, Fiorillo J, Lukacs NW, Kunkel SL, North R, Gerard C, Rollins BJ. Abnormalities in monocyte recruitment and cytokine expression in monocyte chemoattractant protein 1-deficient mice. J Exp Med. 1998; 187:601–608. [PubMed: 9463410]
29. Luster AD, Unkeless JC, Ravetch JV. Gamma-interferon transcriptionally regulates an early-response gene containing homology to platelet proteins. Nature. 1985; 315:672–676. [PubMed: 3925348]
30. Thum T, Gross C, Fiedler J, Fischer T, Kissler S, Bussen M, Galuppo P, Just S, Rottbauer W, Frantz S, Castoldi M, Soutschek J, Koteliansky V, Rosenwald A, Basson MA, Licht JD, Pena JT, Rouhanifard SH, Muckenthaler MU, Tuschl T, Martin GR, Bauersachs J, Engelhardt S. MicroRNA-21 contributes to myocardial disease by stimulating MAP kinase signalling in fibroblasts. Nature. 2008; 456:980–984. [PubMed: 19043405]
31. Medina PP, Nolde M, Slack FJ. OncomiR addiction in an in vivo model of microRNA-21-induced pre-B-cell lymphoma. Nature. 2010; 467:86–90. [PubMed: 20693987]

32. Hatley ME, Patrick DM, Garcia MR, Richardson JA, Bassel-Duby R, van Rooij E, Olson EN. Modulation of K-Ras-dependent lung tumorigenesis by MicroRNA-21. Cancer Cell. 2010; 18:282–293. [PubMed: 20832755]
33. Liu G, Friggeri A, Yang Y, Milosevic J, Ding Q, Thannickal VJ, Kaminski N, Abraham E. miR-21 mediates fibrogenic activation of pulmonary fibroblasts and lung fibrosis. J Exp Med. 2010; 207:1589–1597. [PubMed: 20643828]
34. Boehm U, Klamp T, Groot M, Howard JC. Cellular responses to interferon-gamma. Annu Rev Immunol. 1997; 15:749–795. [PubMed: 9143706]
35. Sheedy FJ, Palsson-McDermott E, Hennessy EJ, Martin C, O'Leary JJ, Ruan Q, Johnson DS, Chen Y, O'Neill LA. Negative regulation of TLR4 via targeting of the proinflammatory tumor suppressor PDCD4 by the microRNA miR-21. Nat Immunol. 2010; 11:141–147. [PubMed: 19946272]
36. Meng F, Henson R, Lang M, Wehbe H, Maheshwari S, Mendell JT, Jiang J, Schmittgen TD, Patel T. Involvement of human micro-RNA in growth and response to chemotherapy in human cholangiocarcinoma cell lines. Gastroenterology. 2006; 130:2113–2129. [PubMed: 16762633]
37. Frankel LB, Christoffersen NR, Jacobsen A, Lindow M, Krogh A, Lund AH. Programmed cell death 4 (PDCD4) is an important functional target of the microRNA miR-21 in breast cancer cells. J Biol Chem. 2008; 283:1026–1033. [PubMed: 17991735]
38. Gunzl P, Schabbauer G. Recent advances in the genetic analysis of PTEN and PI3K innate immune properties. Immunobiology. 2008; 213:759–765. [PubMed: 18926291]
39. Pedroza-Gonzalez A, Xu K, Wu TC, Aspord C, Tindle S, Marches F, Gallegos M, Burton EC, Savino D, Hori T, Tanaka Y, Zurawski S, Zurawski G, Bover L, Liu YJ, Banchereau J, Palucka AK. Thymic stromal lymphopoietin fosters human breast tumor growth by promoting type 2 inflammation. J Exp Med. 2011; 208:479–490. [PubMed: 21339324]
40. De Monte L, Reni M, Tassi E, Clavenna D, Papa I, Recalde H, Braga M, Di Carlo V, Doglioni C, Protti MP. Intratumor T helper type 2 cell infiltrate correlates with cancer-associated fibroblast thymic stromal lymphopoietin production and reduced survival in pancreatic cancer. J Exp Med. 2011; 208:469–478. [PubMed: 21339327]

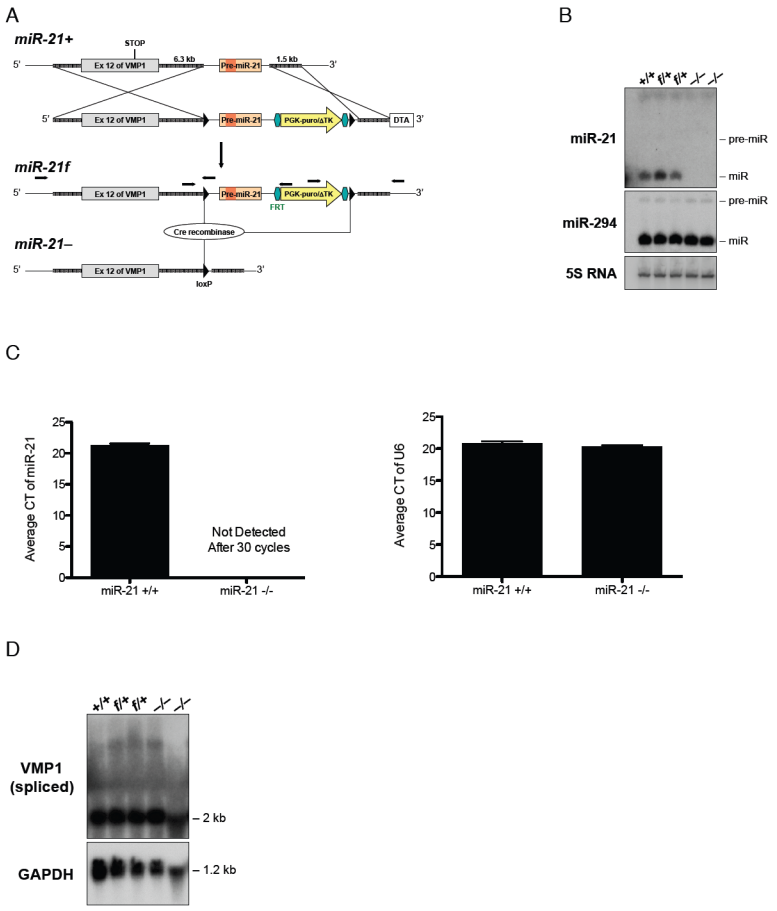


**Figure 1. Generation of miR-21 deficient mice**

(A) Representation of genomic sequence encompassing *Tmem49* (*VMP1*) exon 12 and pre-miR-21 of the miR-21 wild-type (*miR-21*$^{+}$) and targeted alleles before (*miR-21*$^{f}$) and after (*miR-21*$^{-}$) Cre recombinase-mediated excision of the pre-miR-21 containing conditional sequence. Exon 12 contains the translational stop codon (STOP) of *Tmem49*. 6.3 kb of 5' and 1.5 kb of 3' homologous sequence in the targeting vector are represented by thickened gray lines; loxP sites (black triangles) flank pre-miR-21-containing conditional sequence and an FRT site (green hexagon)-flanked pgk-*puroΔTk* gene (yellow arrow) are as indicated. The miR-21 deficient (*miR-21*$^{-}$) allele was derived from the conditional miR-21 (*miR-21*$^{f}$) allele by transient expression of Cre recombinase in gene-targeted embryonic stem (ES) cells. Positions of oligonucleotide pairs (black arrows) used to confirm correct homologous recombination at the miR-21 gene by locus-specific PCR are indicated. (B) Northern analysis of pre- and mature miR-21, pre- and mature miR-294 mRNA in miR-21 wild-type (+/+), heterozygous conditional (f/+), and homozygous gene-targeted (-/-) CJ7 ES cells. The 5S RNA was used as a loading control. (C) Expression level of mature miR-21 from lungs of miR-21$^{+/+}$ and miR-21$^{-/-}$ mice as determined by qRT-PCR; CT: cycle threshold. The U6 small nuclear RNA was used as control. (D) Northern analysis of *Tmem49* (*VMP1*) expression in miR-21 wild-type (+/+), heterozygous conditional (f/+), and homozygous gene-targeted (-/-) CJ7 ES cells using *GAPDH* as loading control. MiR-21$^{-/-}$ ES cells were derived from miR-21$^{f/+}$ ES cells (after Flp recombinase-mediated selection marker removal) through miR-21 re-targeting followed by Cre-mediated excision of the conditional sequence in miR-21$^{f/f}$ cells.

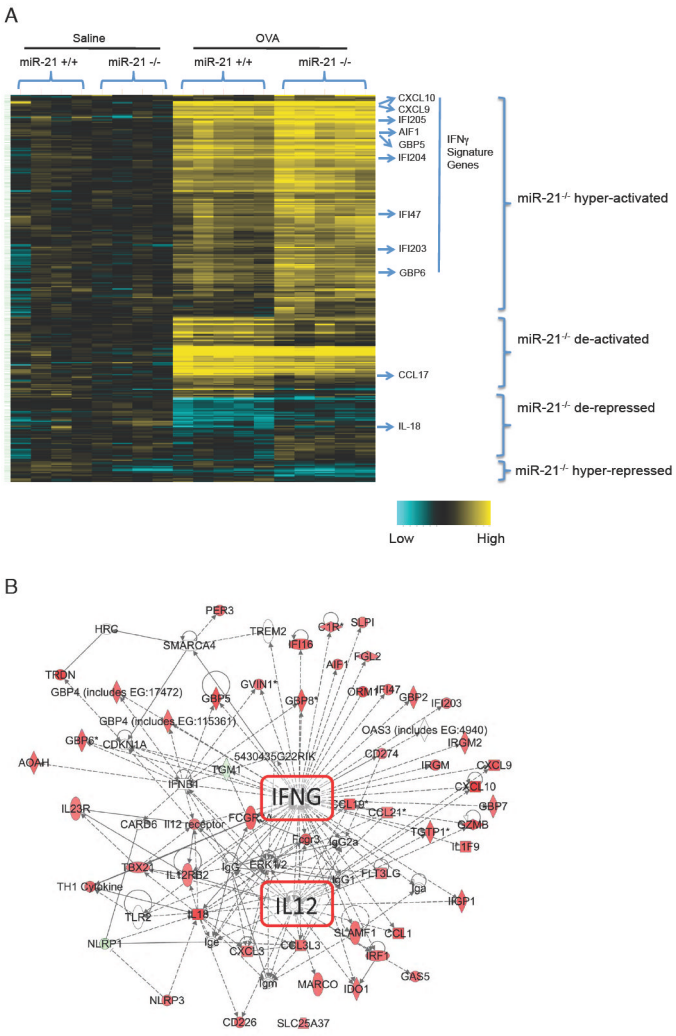

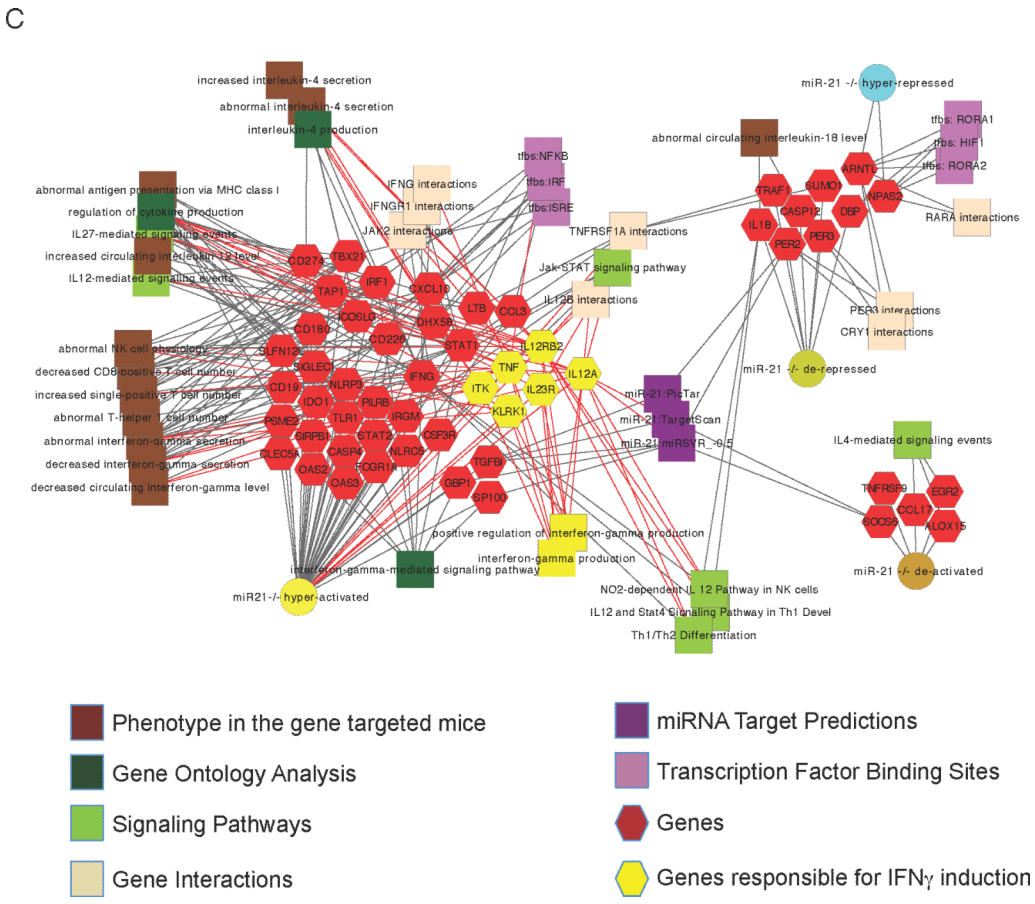


**Figure 2. Heatmap and pathway analysis of differentially expressed genes between miR-21$^{+/+}$ and miR-21$^{-/-}$ lungs before and after OVA challenge**

(A) Hierarchical clustering of genes differentially expressed in the miR-21$^{+/+}$ vs. miR-21$^{-/-}$ lungs after saline or OVA challenge. (B) An up-regulated IL-12/IFNγ pathway identified by Ingenuity Pathway Analysis from all of the genes differentially expressed between miR-21$^{+/+}$ and miR-21$^{-/-}$ OVA-challenged lungs; red color = up-regulated in miR-21$^{-/-}$ vs. miR-21$^{+/+}$ OVA-challenged lungs, green color = down-regulated in miR-21$^{-/-}$ vs. miR-21$^{+/+}$ OVA-challenged lungs. (C) Extensive enrichment of genes with functional features associated with antigen presentation and T cell polarization among genes whose expression is altered by loss of miR-21 in saline- and OVA-treated mouse lungs. The network is shown as a Cytoscape graph network generated from ToppCluster network analysis. Each expression pattern gene cluster from Panel A is represented as a node connected to some of the top-ranked genes of each cluster that share enriched properties and biological features. Genes that are key activators of pathways responsible for IFNγ induction are shown as yellow rather than red hexagons, and their respective feature and function relationships are shown connected via red edges. The features that are highly significant for other genes in the cluster are connected by gray edges. For example, mouse targeted gene disruption phenotypes (brown square nodes) of a large number of these genes give phenotypes in mice that cause increased IL-4 expression and/or decreased IFNγ production.

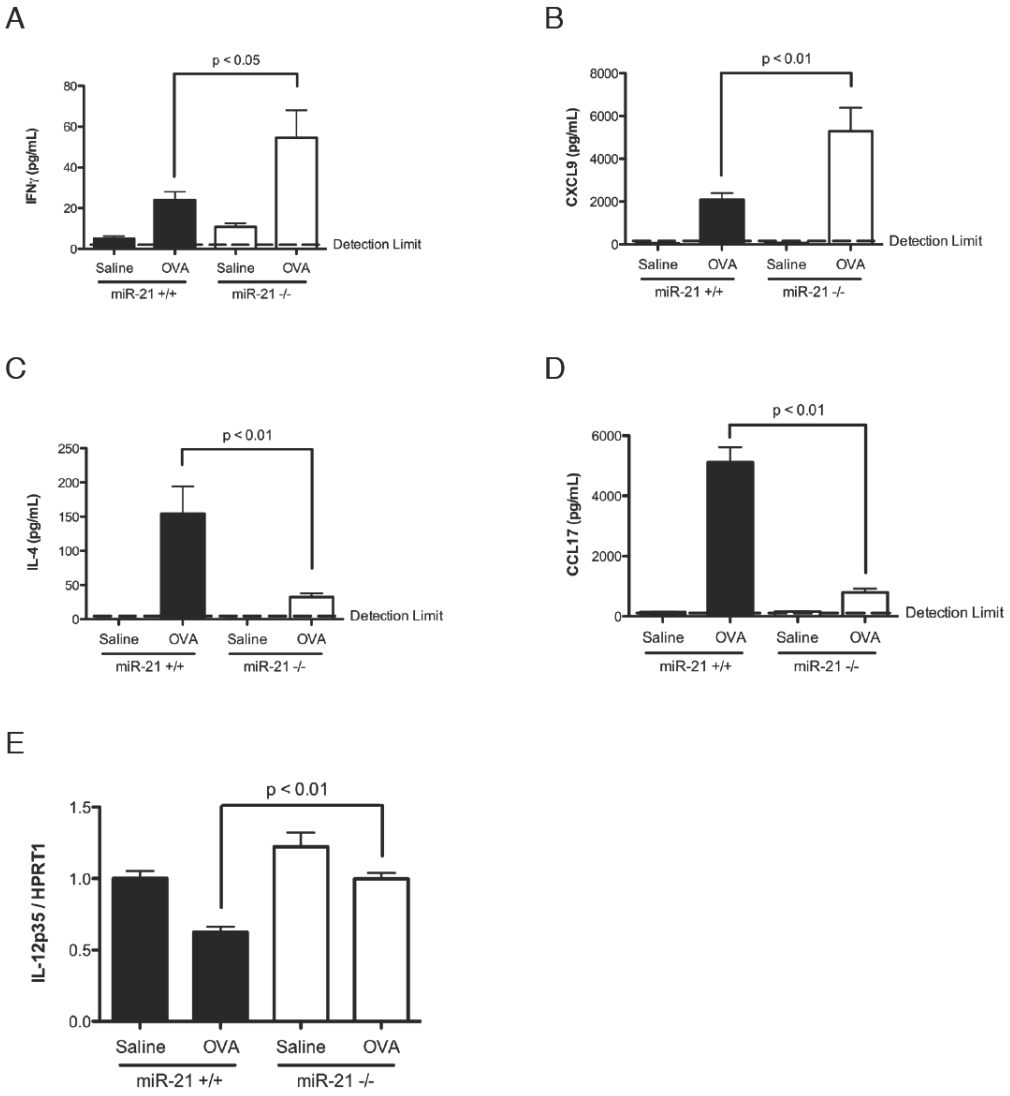


**Figure 3. Cytokine expression level in lung and bronchoalveolar lavage fluid (BALF) of allergen-challenged miR-21$^{+/+}$ and miR-21$^{-/-}$ mice**

Levels of (A) IFNγ, (B) CXCL9, (C) IL-4, and (D) CCL17 in the BALF of OVA-challenged miR-21$^{-/-}$ mice and miR-21$^{+/+}$ littermate controls as determined by ELISA. (E) Expression level of IL-12p35 in the lungs of OVA-challenged miR-21$^{-/-}$ mice and miR-21$^{+/+}$ littermate controls as determined by qRT-PCR normalized to *HPRT1*. Data are represented as mean ± S.E.M.; n = 6-15 mice per group; data representative of three independent experiments.

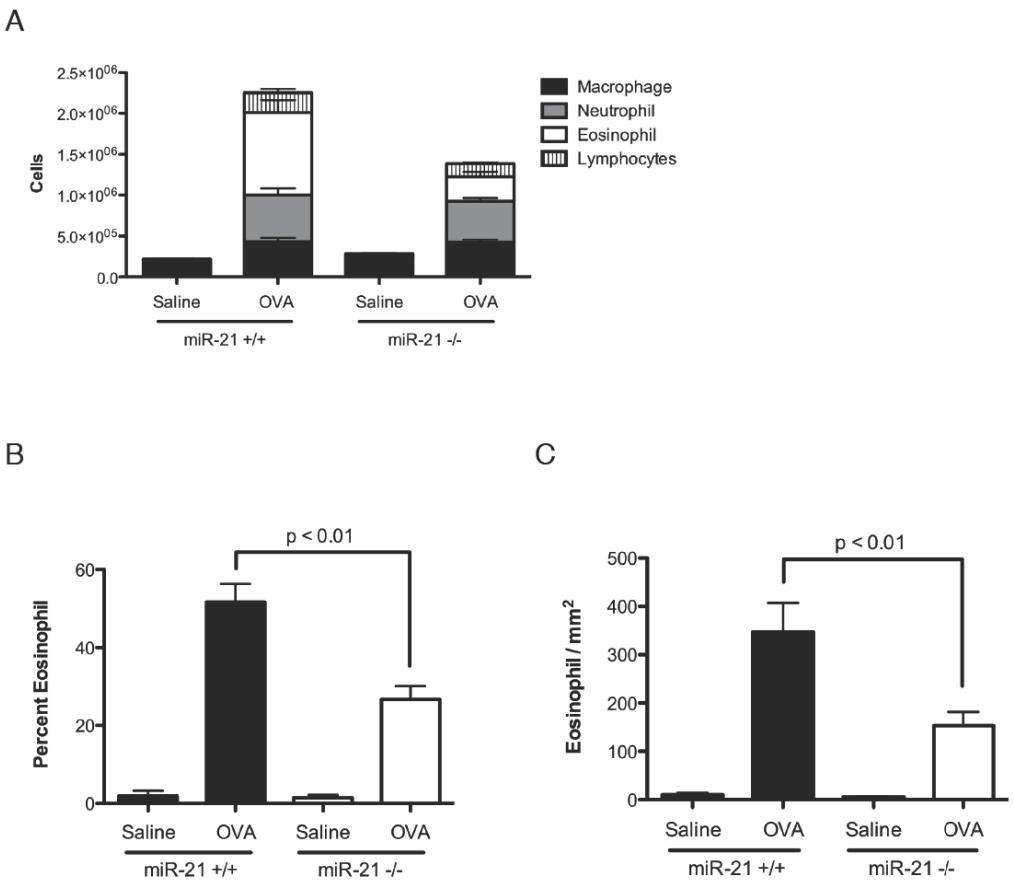


**Figure 4. Eosinophil levels in the bronchoalveolar lavage fluid (BALF) and in the lung after OVA allergen challenge**

(A) Total and differential BALF cell counts. (B) Percentages of eosinophils in the BALF. (C) Eosinophil infiltration in the lung tissue. Data are represented as mean ± S.E.M.; n = 5-10 mice per group; data representative of three independent experiments.

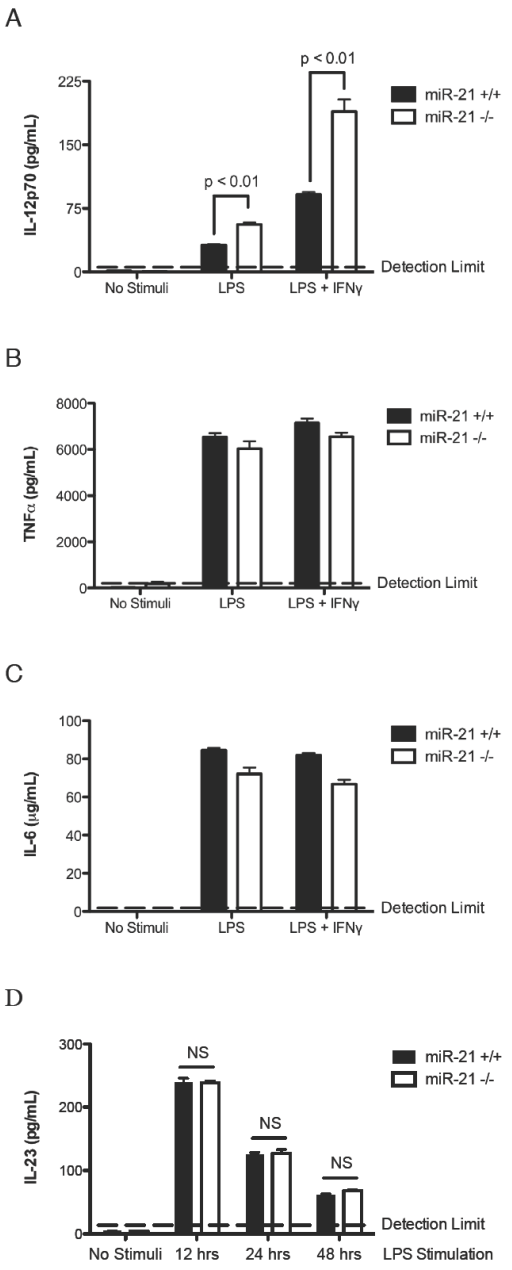


**Figure 5. IL-12p70 production by LPS stimulated miR-21$^{+/+}$ and miR-21$^{-/-}$ dendritic cells in the presence and absence of IFNγ**

Bone marrow-derived dendritic cells were cultured from miR-21$^{-/-}$ mice and miR-21$^{+/+}$ littermate controls. (A) IL-12p70, (B) TNFα, and (C) IL-6 levels were measured by ELISA from the supernatant of dendritic cells stimulated with 1 μg/mL LPS alone or 1 μg/mL LPS plus 100 IU/mL IFNγ. (D) IL-23 levels were measured by ELISA from the supernatant of dendritic cells stimulated with 1 μg/mL LPS for 12, 24 or 48 hrs. NS: Not Significant. Data are represented as mean ± S.E.M.; n = 4 per group; data representative of three independent experiments for panel A-C, data representative of two independent experiments for panel D.

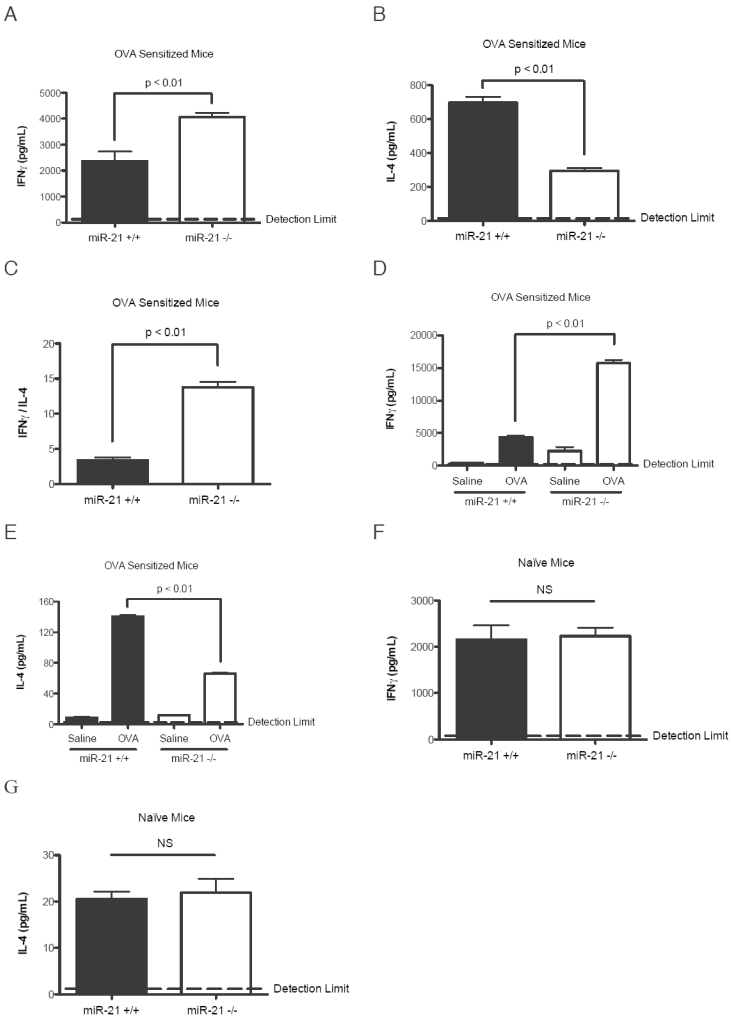


**Figure 6. Cytokine levels after re-stimulation of splenic CD4$^+$ lymphocytes from naïve or OVA challenged miR-21$^{+/+}$ and miR-21$^{-/-}$ mice**

Levels of (A) IFNγ and (B) IL-4 after anti-CD3/CD28 re-stimulation of purified splenic CD4$^+$ T lymphocytes from OVA-challenged miR-21 $^{+/+}$ and miR-21$^{-/-}$ mice as measured by ELISA. (C) Ratio of IFNγ to IL-4. (D) Levels of IFNγ and (E) IL-4 after saline or OVA re-stimulation of total splenocytes from OVA-challenged miR-21$^{+/+}$ and miR-21$^{-/-}$ mice as measured by ELISA. (F) Levels of IFNγ and (G) IL-4 after anti-CD3/CD28 re-stimulation of purified splenic CD4$^+$ T lymphocytes from naïve miR-21$^{+/+}$ and miR-21$^{-/-}$ mice as measured by ELISA.NS: Not Significant. Data are represented as mean ± S.E.M.; n = 3-4 per group; data representative of three independent experiments for panel A-C, data representative of two independent experiments for panel D-G.

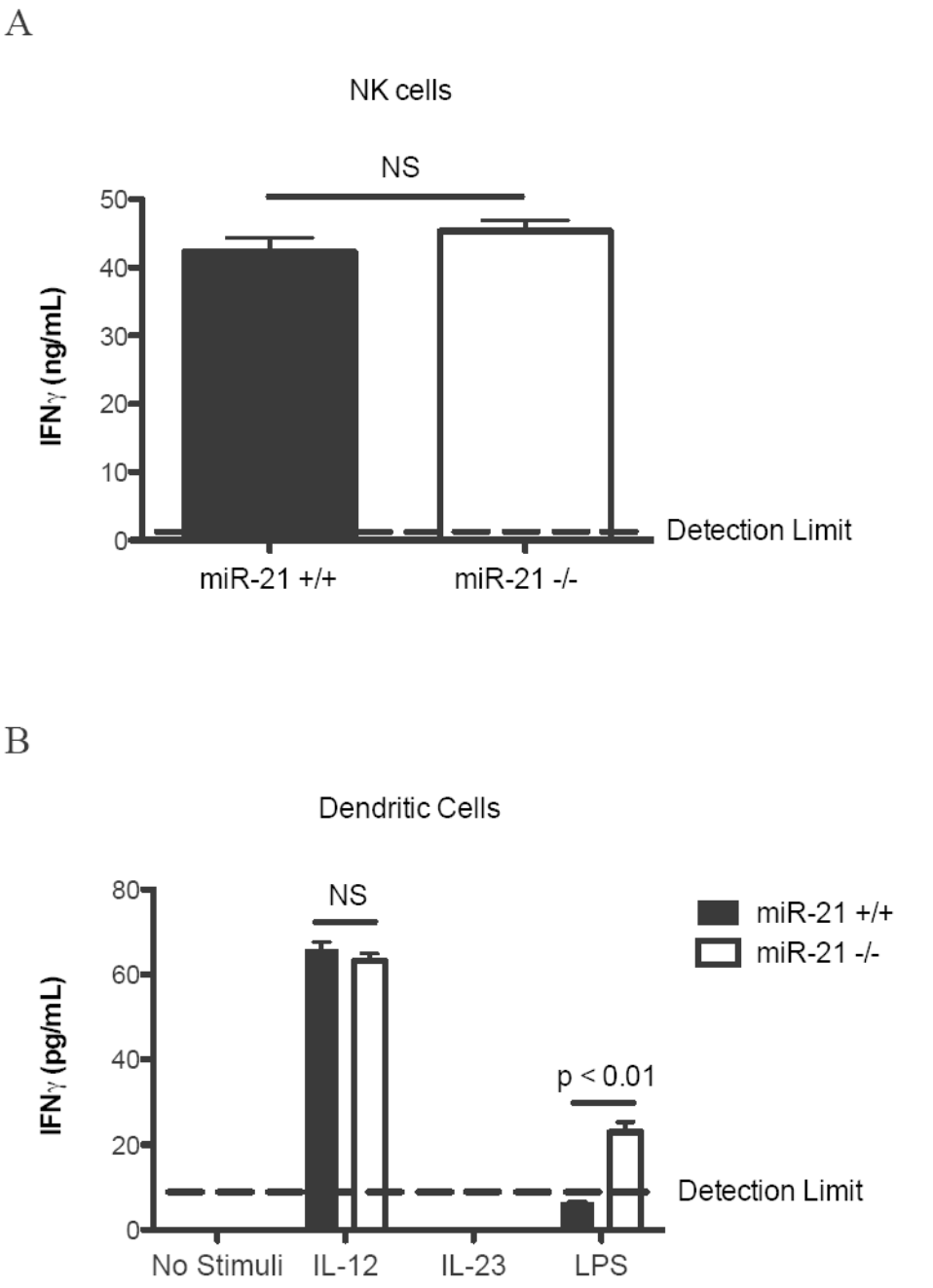


**Figure 7. IFNγ production by IL-12 stimulated NK cells and IL-12, IL-23 or LPS stimulated dendritic cells from miR-21$^{+/+}$ and miR-21$^{-/-}$ mice**

**(A)** NK cells were purified from the spleen of miR-21$^{+/+}$ and miR-21$^{-/-}$mice. IFNγ levels were measured by ELISA from the supernatant of NK cells stimulated with 10 ng/mL IL-12. (B) Bone marrow-derived dendritic cells were cultured from miR-21$^{-/-}$ mice and miR-21$^{+/+}$ littermate controls. IFNγ levels were measured by ELISA from the supernatant of dendritic cells stimulated with 10 ng/mL IL-12, 10 ng/mL IL-23, or 1 μg/mL LPS. NS: Not Significant. Data are represented as mean ± S.E.M.; n = 4 per group; data representative of two independent experiments.

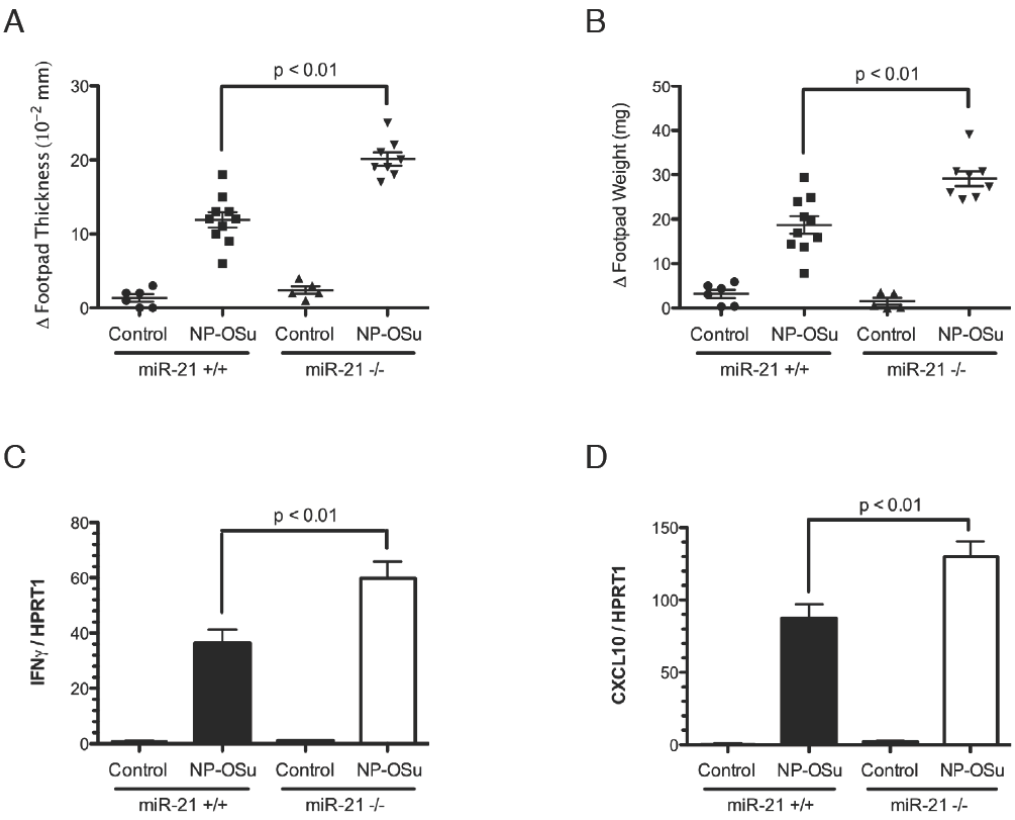


**Figure 8. Footpad swelling and cytokine levels of miR-21$^{+/+}$ and miR-21$^{-/-}$ mice in a NP-OSu-mediated cutaneous delayed-type hypersensitivity model**

Changes in (A) footpad thickness and (B) footpad weight after NP-OSu challenge in miR-21$^{-/-}$ mice compared to wild-type littermates. (C) Expression levels of IFNγ and (D) CXCL10 in the footpad of NP-OSu-challenged miR-21$^{-/-}$ mice and miR-21$^{+/+}$ littermate controls as determined by qRT-PCR normalized to *HPRT1*. Data are represented as mean ± S.E.M.; n = 5-10 mice per group; data representative of three independent experiments.

**Table I**

Functional enrichment analysis of miR-21 dysregulated genes in the allergen-challenged murine lung compared with miR-21 co-regulated genes in human samples

| | | | Mouse[a] (247 genes) | | Human[b] (182 genes) | |
|---|---|---|---|---|---|---|
| **Category** | **Name** | **Genes in Genome[c]** | **Query genes in Category** | **P-value** | **Query genes in Category** | **P-value** |
| GO: Biological Process | immune system process | 1450 | 65 | $10^{-22}$ | 58 | $10^{-22}$ |
| GO: Biological Process | defense response | 905 | 55 | $10^{-25}$ | 38 | $10^{-15}$ |
| GO: Biological Process | cytokine-mediated signaling pathway | 234 | 19 | $10^{-11}$ | 17 | $10^{-11}$ |
| Human Phenotype | immunological abnormality | 297 | 13 | $10^{-4}$ | 10 | $10^{-3}$ |
| Mouse Phenotype | altered susceptibility to infection | 373 | 34 | $10^{-15}$ | 25 | $10^{-8}$ |
| Mouse Phenotype | abnormal cell-mediated immunity | 1008 | 47 | $10^{-10}$ | 57 | $10^{-16}$ |
| Mouse Phenotype | abnormal antigen presenting cell | 663 | 34 | $10^{-8}$ | 46 | $10^{-16}$ |
| Transcription Factor Binding | NFkB | 210 | 8 | $10^{-3}$ | 12 | $10^{-5}$ |
| Co-expression | down-regulated in monocyte-derived dendritic cells after stimulation | 452 | 29 | $10^{-14}$ | 21 | $10^{-9}$ |

[a] Lung;

[b] Co-regulated genes in the human samples. Analysis was performed using the Toppcluster suite.